

# Section 1

## THE OMEGA UPGRADE

### 1.A OMEGA Upgrade System Design Update

The OMEGA Upgrade Preliminary Design Document (Title I document), which was submitted to DOE in October 1989, set forth the design objectives and specifications for a laser system capable of delivering approximately 30 kJ of energy onto a fusion target, and presented a design that would meet them.<sup>1</sup> Since that document was issued, the design of the OMEGA Upgrade has undergone several changes as a result of ongoing analysis. Some of the changes were necessary reconfigurations in the system layout while others were refinements of detailed design. The changes described herein have not altered the specifications to which the laser must perform, and these are summarized in Table 44.I.

The primary design change occurred in the configuration of the beam-transport system, which is all of the optical components between the frequency-conversion crystals and the target. This change was necessary to reduce the possibility of generating stimulated rotational Raman scattering (SRRS) in the high-powered 351-nm beams. The difference between the old and new beam-transport configurations is evident in the comparison of Fig. 44.1 and Fig. 44.2. In the new configuration the beams pass through the blue relays and straight into the target bay, eliminating the end and injection mirrors that were located in the laser bay. This raises the intensity threshold for SRRS in two ways: a reduction in the path length in air from the frequency-conversion crystals to target by the addition of blue relays, which provide a long vacuum path, and the reduction of beam fluence due

to the 1.15X magnification of the relays. The stage C-D beam-splitting area was reconfigured in order to reduce the potential of mirror damage due to beam modulations induced by smoothing by spectral dispersion (SSD). This new system layout also allows room for the oscillators and driver lines in the laser bay. (The previous design placed these systems in the capacitor bay below the laser bay.) Additional changes that result from this reconfiguration will be outlined here as well.

Table 44.I: Performance goals of the OMEGA Upgrade system.

	Main Pulse		Foot Pulse	
	Beam area (cm <sup>2</sup> )	321		71
Temporal shape	Gaussian		Half-Gaussian	
Crystal thickness $L$ (cm)	0.76		1.6	
UV FWHM (ns)	0.50	0.75	3.0	5.0
IR FWHM (ns)	0.56	0.9	3.3	5.56
Nominal IR intensity on crystal $I_0$ (GW/cm <sup>2</sup> )	5.47	3.38	0.98	0.98
Normalized IR intensity of most intense ray <sup>(a)</sup>	5.14	3.18	4.08	4.08
Operating point of most intense ray <sup>(b)</sup>	$M_1$	$M_2$	$F$	$F$
Frequency-conversion efficiency (%)	80	70	75	75
IR energy-per-beam on to crystals (J)	977	977	116	194
UV energy-per-beam out of crystals (J)	782	684	87	146
UV energy-per-beam on target (J) <sup>(c)</sup>	564	493	62.7	105
Average UV energy loading after crystals (J/cm <sup>2</sup> )	2.4	2.1	1.2	2.1
AR damage fluence for full Gaussian (J/cm <sup>2</sup> )	3.8		6.8	
Peak UV power on target (TW)	63.5	37.1	2.4	2.4
Total UV energy on target (kJ)	33.8	29.6	3.8	6.3
Truncated UV energy on target (kJ) <sup>(d)</sup>	27.1	23.7	3.8	6.3

(a)  $0.9394 I_0 (L/0.76)^2$ . See Fig. 39.3, LLE Review 39, 120 (1989).  
 (b) See Fig. 39.3, LLE Review 39, 120 (1989).  
 (c) Assumes a 9% transport loss and a DPP efficiency of 79% (into the central disk of the focal spot).  
 (d) With truncation of the last 20% of the main-pulse UV energy.

TC2631

### Oscillator and Driver Lines

The redesign of the C and D split area has allowed room in the laser bay for the oscillators and driver lines. They have been moved from the capacitor bays beneath the laser bay up to the main laser-bay floor. The old and new configurations are depicted in Figs. 44.1 and 44.2.

The relocation of these components has reduced the path length between the driver lines and the A split area and has also reduced cost by decreasing the number of optics required.

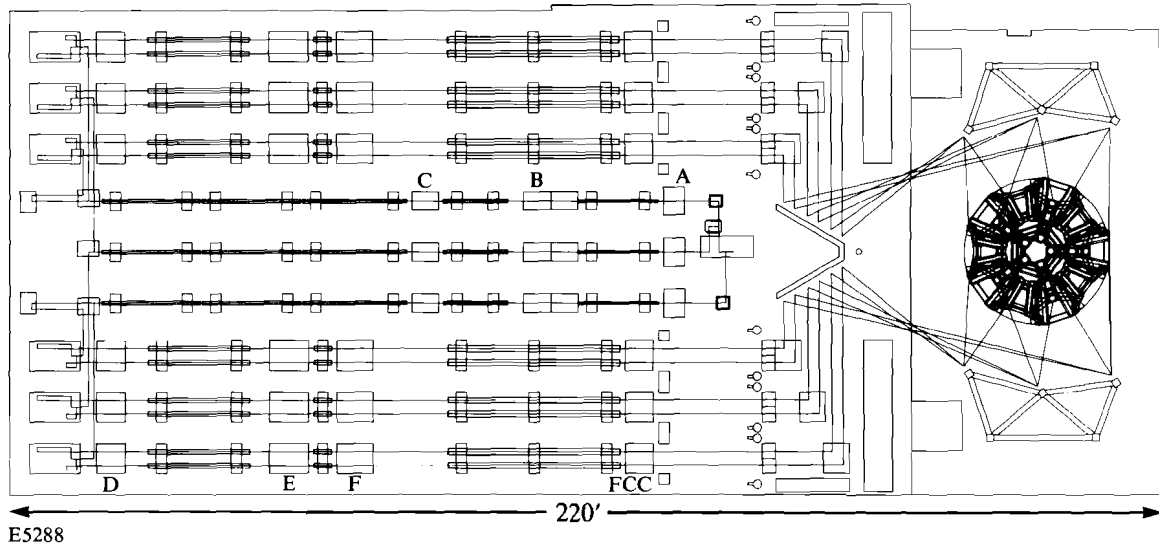


Fig. 44.1  
Old OMEGA Upgrade layout.

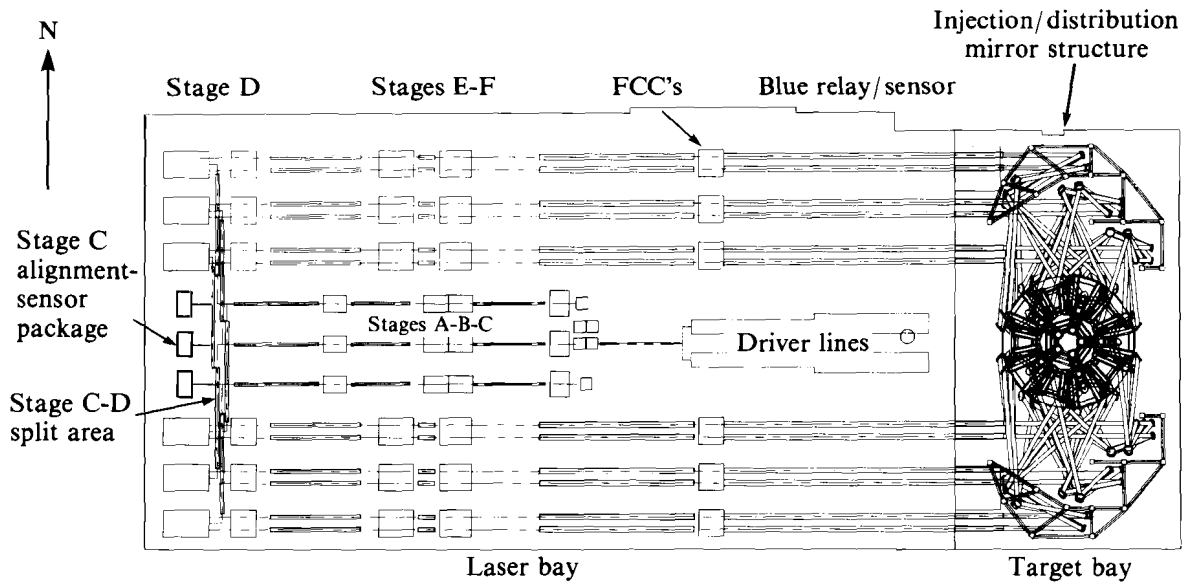


Fig. 44.2  
New OMEGA Upgrade layout.

### C and D Split Area

High-order spatial frequencies from diffraction and SSD modulation effects can cause nonuniformities in the beam (hot spots). If not controlled, the intensity of these hot spots, which increases with the distance from an image plane, can exceed the damage thresholds of the optical coatings used in the OMEGA Upgrade. To reduce the risk of damage from these modulation effects, a new C and D beam-splitting area has been designed that significantly reduces the path length from the relay output lenses to the image planes and eliminates 20 mirrors and their mounts from this portion of the laser system.

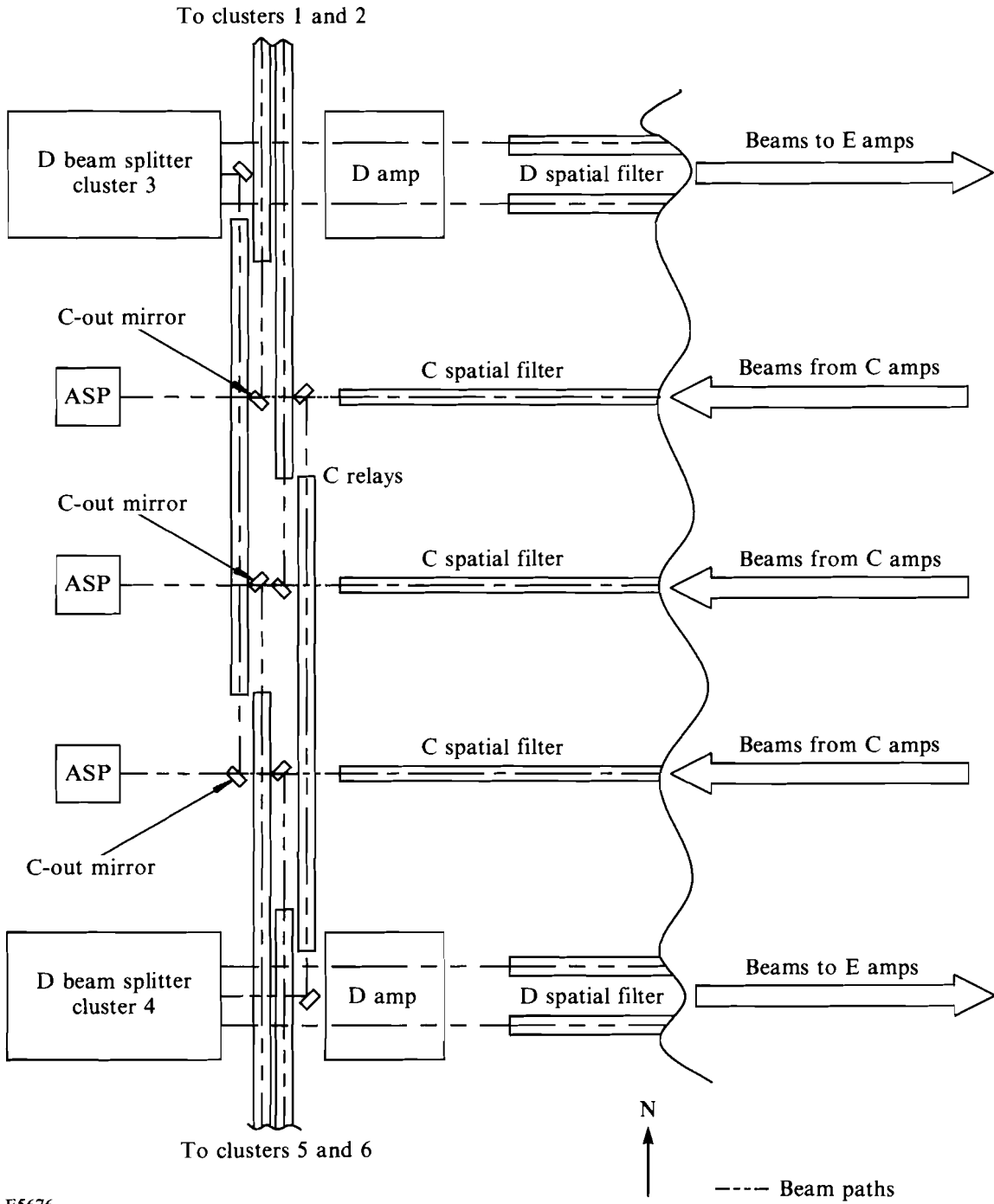
In the new design (see Fig. 44.2), just after the 64-mm stage-B amplifiers, three vertical groups of five beams are relayed to the stage-B spatial filters. These filters magnify each beam by 1.46, then relay them to the 90-mm stage-C amplifiers. After these amplifiers, the stage-C spatial filters relay the beam with no magnification to the stage-C output-mirror structures. At that point, 50% beam splitters divide each beam into two equal components, traveling either north or south and remaining arranged vertically (as shown in Fig. 44.3).

Half of the beams then encounter the stage-C end mirror, which has a 99.5% reflection coefficient. The 0.5% transmitted energy is used for the alignment-sensor package that will be a modified beam-diagnostic package from OMEGA. These alignment-sensor packages will perform alignment and energy measurements in stages A, B, and C. After the 50% beam splitters and the end mirrors, the 30 beams pass through the stage-C 1:1 relays, spatial-filter assemblies without pinholes.

At the output of the driver lines, images from driver-line gratings and apodizers are merged to form a single reference image. This primary image plane is propagated via the spatial filters and relays through the folding and splitting area. This final split divides the 30 beams into 60 beams. The beams are then directed to the stage-D amplifiers while maintaining nominally equal path lengths.

The new configuration requires that four clusters be elevated in order to maintain the shortest path length and to avoid having beams hitting mechanical components. To do this, vertical spacers were added to the appropriate support structures. The layout of the new C and D split area, as seen from floor level facing east, is shown in Fig. 44.4.

This new design has reduced the diffraction modulations at the output of the stage-C relays, and the SSD-induced modulation within the C and D split area has been cut in half. The cost benefit of the new configuration is the elimination of 20 mirrors along with their associated mounts and control systems.



E5676

Fig. 44.3  
 Layout showing the direction of beam propagation and the location of the alignment-sensor packages (ASP's) after the C-mirrors.

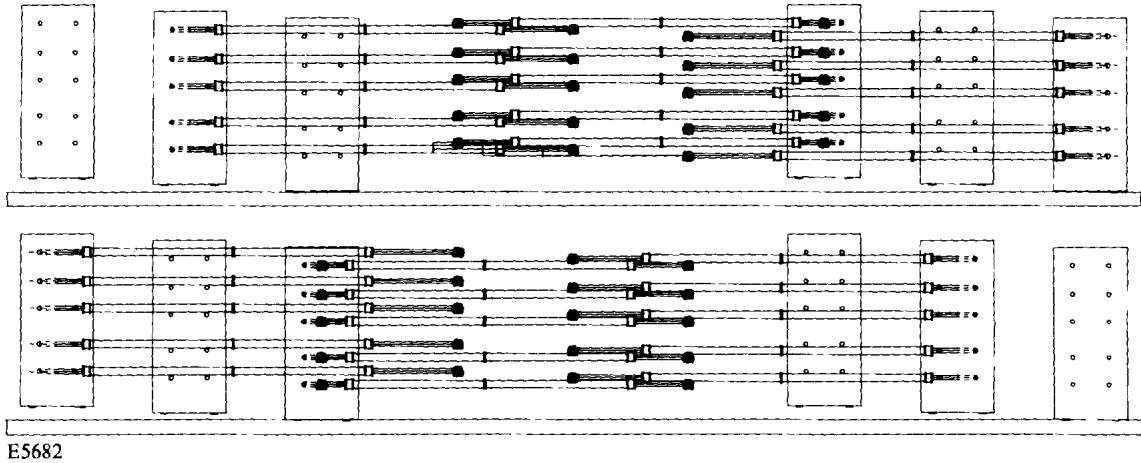


Fig. 44.4  
Stage C and D split area as seen from the alignment-sensor packages (ASP's) looking toward the target bay.

### Beam Transport and Blue Relays

The Title I system configuration shown in Fig. 44.1 has a beam-transport system that emulates the existing OMEGA beam transport and includes four mirrors per beam from the frequency-conversion crystals to the target-focus lenses. The configuration also incorporates all of the necessary alignment and diagnostic sensors in the laser bay. In the new configuration shown in Fig. 44.2, the end mirrors, which fold the beams to the injection mirrors in the center of the laser bay, were eliminated, thus the blue relays could be included in a straight-line configuration. This required a complete reconfiguration of the target-area mirrors, resulting in an injection and distribution mirror per beam in the target bay. The final target mirrors are located on the outside of the target-mirror structure as before. Inclusion of the blue relays also forced the creation of an alignment/diagnostic sensor subsystem that is integrated with the blue relays. An additional objective of the redesign exercise was to keep the number of large optical components per beam to a minimum.

In the original Title I design, the distance in air between the frequency-conversion crystals and the focus lenses was sufficient to possibly allow SRRS to cause an undesirable level of modulation of the beam. In addition, it is desirable to image the frequency-conversion crystals to the target mirrors to reduce the possibility of damage due to SSD modulations. The blue relays, which have a 17-m-long vacuum tube, will reduce SRRS in the UV beams propagated to the target chamber by reducing the total path length in air and by expanding the beam to reduce fluence. These relays transfer the image at the frequency-conversion crystals to a plane between the target mirrors and the focus lenses. In addition to image relaying, the blue relays also support beam alignment and diagnostic sensors. The blue-relay design concept is shown in Fig. 44.5.

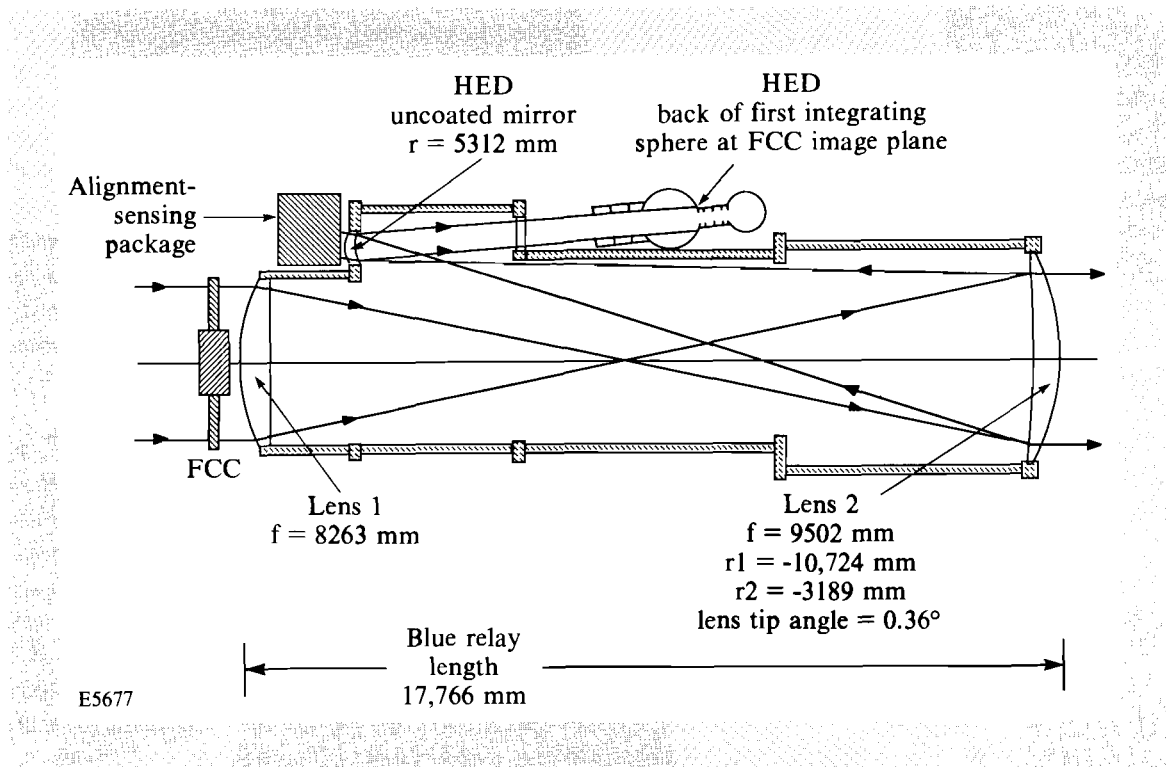


Fig. 44.5  
Diagram of the blue image relays showing the integration of the alignment and harmonic-energy diagnostics.

The threshold for SRRS depends on the product of the beam intensity, the path length in air, and the bandwidth of the beam. The new configuration, which includes the blue relays, reduces the path length in air for the UV beam from 40 m to 23 m and expands the beam by a factor of 1.15 (thus reducing the beam intensity by 25%). These changes have raised the intensity threshold at which SRRS will occur to above the operating intensity of the upgraded OMEGA laser.<sup>2,3</sup>

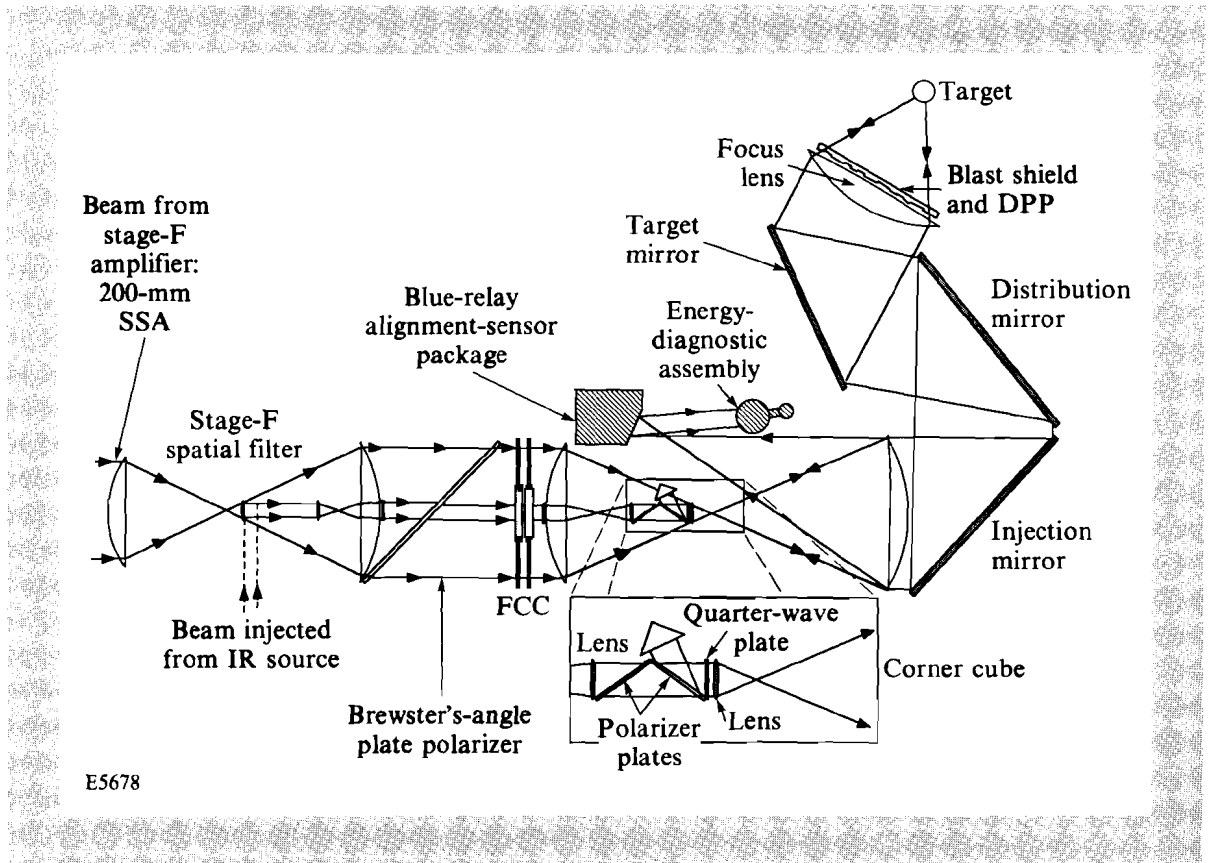
Since the alignment and harmonic-energy diagnostics are incorporated in the blue-relay assemblies, it is not possible to use a pinhole to filter out the higher-order spatial frequencies. Furthermore, the unconverted red and green energy that is nearly focused at the pinhole plane would damage the pinhole and blow off unwanted debris in the vacuum. However, the improvement in the design due to the increase in the SRRS threshold and the elimination of 60 large mirrors far outweighs this drawback.

The alignment-sensor package on the blue relay will be used for beam pointing, centering, and pinhole alignment (at  $1.054 \mu\text{m}$ ) for stages D, E, and F. The blue alignment-sensor package is designed to be achromatic at  $1.054 \mu\text{m}$  and  $0.351 \mu\text{m}$ . Using two-dimensional image sensors, it will detect beam pointing and centering locations, and image processing will be done by the alignment computers. The accuracy will be  $\sim 1 \mu\text{rad}$ , as required for targeting.

The current concept for beam alignment from the frequency-conversion crystals to target uses a continuous-wave (cw), mode-locked, Q-switched, amplified laser, which is frequency tripled at the crystals to provide a UV beam for alignment. Computer-controlled rotating wave plates would be adjusted to send all of this energy down one or two of the beamlines. Auxiliary optics are required in the stage-F spatial filter to down-collimate the beam to achieve the necessary intensity for frequency conversion. Consistency in beam pointing would then be verified using the blue alignment-sensor package. An advantage of this technique would be the ability to check the angle tuning of the frequency-conversion crystals without performing full-system shots.

Once the laser beamlines are aligned in the IR, the UV-alignment beam is co-aligned with the red beam using the blue alignment-sensor package and transported to the target-mirror structure by the injection and distribution mirrors. The specific centering technique for this beam has yet to be determined, but image acquisition and processing will be used to determine its centering accuracy at the target mirror to within  $\pm 1$  mm. Final target alignment can be accomplished by reflecting the beam off the target and back to auxiliary optics located in the focal plane of the blue relay, which then reflect the return beam into the blue alignment-sensor package. The auxiliary optics could consist of a polarizer, a quarter-wave plate, and a corner-cube reflector, as shown in Fig. 44.6.

Fig. 44.6  
Alignment-sensing strategy showing the arrangement of the corner-cube assembly.





### Harmonic-Energy Diagnostics

In order to monitor system performance, it will be necessary to separately measure the energy of the main and foot pulses in the co-propagated beam. The alignment-sensor packages, located after the stage-C end mirrors, will use calorimeters to separately measure the whole-beam IR energy in the foot and main pulses. Energy measurements made after the frequency-conversion crystals will be performed with the harmonic-energy diagnostics, a new version of the existing multiwavelength energy-sensing system<sup>4</sup> that utilizes two separate but coaxial integrating spheres, one each for the main and foot pulses. To meet the energy-balance specifications for the laser, the diagnostics must provide measurements of the UV energy on target that have an accuracy of 1%–2%. For power balance, the performance of the frequency-conversion crystals must also be monitored. To do this, the harmonic-energy diagnostics must measure the IR, green, and UV energies emerging from the crystals. A 4% reflection of the beam, from the first surface of the blue-relay output lens, will be injected into an integrating sphere containing four detectors with filters selected to measure each of three wavelengths: 0.351  $\mu\text{m}$ , 0.527  $\mu\text{m}$ , and 1.054  $\mu\text{m}$ . At 0.351  $\mu\text{m}$ , two detectors will supply redundant measurements.

The calibration of the harmonic-energy diagnostics will be accomplished using the SCI-Tech volume-absorbing calorimeters currently used as references in OMEGA. This technique involves tuning the frequency-conversion crystals to IR and using that beam-energy measurement as a baseline for successive measurements as the frequency-conversion crystals are tuned to green and UV.

### Coatings

The laser system contains a large number of optics that require various types of coatings on one or more surfaces. Ongoing work in the Thin Film Technologies Group has demonstrated the ability to deposit coatings on small optics with damage thresholds satisfying the requirements of the laser system.<sup>5</sup> Viable designs have also been conceived for the transport optics and distributed phase plates. The article in Section 2 of this issue provides an in-depth report on the advances in those technologies.

### Power Conditioning

The new power-conditioning system will provide significantly improved control of individual amplifiers than that currently used on OMEGA. While employing new approaches and designs, much of the existing OMEGA hardware will be reused. Each power-conditioning unit will have its own charging supply to facilitate individual control of the charge voltage. Instructions will be relayed from a single-host computer, via a three-conductor fiber-optic network, to a micro-controller located in each power-conditioning unit. The fiber-optic network has three lines: a communications line, an interlock line (the Ready Line), and a fire-synchronization-signal line. The power-conditioning units will be organized as eight groups connected in individual loops to serial ports on the host computer. One loop will control the driver lines, the second will control the stages-A–C

amplifiers, and the other six will each control a single cluster of the stages-D-F amplifiers. Each micro-controller will be able to monitor interlock and status signals and relay that information back to the host computer.

In addition to building new rod power-conditioning units, existing OMEGA rod units will be modified to incorporate individual chargers and micro-controllers. For the single-segmented amplifiers, the design will be similar except that pre-ionization lamp-check circuits will be added. The specification for the single-segmented amplifier pulse-forming networks (PFN) are shown in Table 44.II.

Table 44.II: Specifications for the single-segmented amplifier (SSA), pulse-forming networks (PFN's).

		15-cm Amplifier	20-cm Amplifier
Linear resistance	(m $\Omega$ )	120	120
Pulse width	( $\mu$ s)	550	550
Inductance	( $\mu$ H)	160	160
Capacitance	(mF)	210	210
Charge voltage	(V)	14,162	14,102
Stored energy			
PFN	(J)	21,059	20,881
head	(J)	252,708	334,096

E5684

### Control Systems

The OMEGA Upgrade will require over 2000 control channels for devices such as mirrors, positioners, shutters, etc. There are three main groups of devices to be controlled: two-state devices such as shutters and flip-ins; single-motor devices such as rotating wave plates; and dual-motor devices such as pinhole manipulators and mirror positioners. The current OMEGA alignment system is based on a computer-automated measurement and control (CAMAC) interface that employs multiplexed stepper-motor drivers to control the analog devices and digital input/output (I/O) devices to control the two-state devices. With ten times more devices to control, this approach becomes impractical due to the cost of cable installation and maintenance alone.

Several alternative approaches have been considered in terms of function and expense. The three most viable systems are a distributed CAMAC system, a distributed VERSAbus Motorola European (VME) system, and a serial network consisting of custom intelligent local device controllers.

An analysis of these systems shows that the serial network has significant cost advantages over the other two configurations; the primary savings are from the substitution of dc motors for stepper motors and the reduction of cabling requirements.

The serial network would be the backbone for a number of small, strategically positioned networks in the laser and target bays. Each intelligent controller would be linked to the network by low-cost coaxial cable, which is also simple to install. Each major device type will have a controller that employs a standard communications protocol being developed at LLE. A proposed layout is shown in Fig. 44.7.

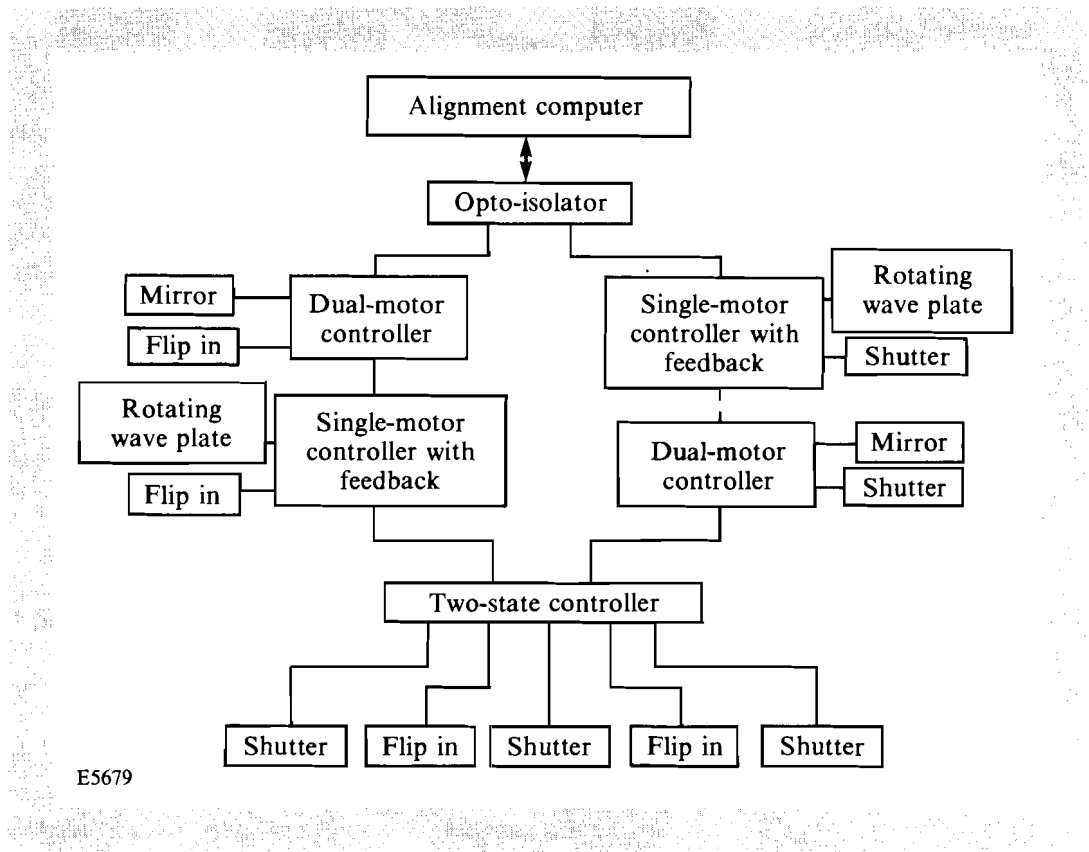


Fig. 44.7  
Functional diagram of the control-system strategy using a serial loop.

In contrast to the systems currently in use, the new controllers will continuously monitor, report, and adjust the state of the device each controls. A clear advantage is simplicity since any anomalous behavior of the device is handled by the local controller without intervention of the host computer, which is ultimately notified via the serial network. This will greatly improve the response time to these events and relieve the host computer of most of the control processing. The serial nature of the network lends itself to easy expansion; adding a device is simply a matter of connecting the new device to the network and adding a subroutine to the host control program.